ELSEVIER

Journal of Structural Geology 29 (2007) 1327–1338

JOURNAL OF STRUCTURAL GEOLOGY

www.elsevier.com/locate/jsg

Melt-assisted interior to margin switch from dislocation to diffusion creep in coarse grained plagioclase: Evidence from a deformed anorthosite pluton

P. Nasipuri, A. Bhattacharya*

Department of Geology and Geophysics, Indian Institute of Technology, Kharagpur 721302, West Bengal, India

Received 7 September 2006; received in revised form 18 April 2007; accepted 19 April 2007
Available online 5 May 2007

Abstract

At Bolangir (Eastern India), massive anorthosites in the pluton interior grade into anorthosites with outward-dipping, margin-parallel foliation neighboring the pluton margin. Sheets and veins of ferrodiorites – residual melts of anorthosite crystallization – concordant and discordant to the margin-parallel foliation suggest pluton deformation at near magmatic conditions, T ~ 950 °C and P 6–12 kbar. In the pluton interior, the larger-than-centimeter sized magmatic plagioclase grains are replaced by aggregates of smaller (100–600 μm) dynamically recrystallized internally-strained grains with un-equilibrated boundaries. Neighboring the pluton margin, poly-sized (200–2500 μm) plagioclase grains in anorthosites are of two types: strain-free rectangular-shaped plagioclase grains with high-energy An-richer margins indenting neighboring plagioclase grains formed by diffusion creep, whereas unstrained end-to-end touching euhedral plagioclase grains showing tilling represent magmatic flow textures. The pluton interior-to-margin switch in plagioclase deformation from grain boundary migration accommodated dislocation creep to grain boundary diffusion creep is attributed to the increasing melt fraction (melt/crystal ratio) during syn-deformation pluton emplacement. Plagioclase grains in the Bolangir pluton are significantly coarser compared to plagioclase aggregates (<200 μm) in experiments designed to understand deformation mechanisms. The present study demonstrates that presence of melts promoted diffusion creep over dislocation creep, albeit in larger-than-experiment plagioclase grains.

Keywords: Anorthosite; Plagioclase; Diffusion creep; Dislocation creep; Melt-wetting

1. Introduction

Experiments with natural and synthetic plagioclase (An_{0-100}) at varying shear stress (1–2000 MPa), strain rate ($2.5 \times 10^{-4}\ s^{-1}$–$20 \times 10^{-6}\ s^{-1}$) and temperature (900–1365 °C) in dry and wet (<0.9 wt% H_2O) conditions (Dell' Angelo et al., 1987; Dimanov et al., 1998, 1999, 2000; Huang et al., 2001; Rybacki and Dresen, 2000; Tullis and Yund, 1985, 1991, 1992; Wang et al., 1996) indicate dislocation and diffusion-controlled creeps to be the preferred mechanisms by which plagioclase deform at lower crustal temperature. Smaller grain size, at high temperature, low shear stress and strain rate (Rybacki and Dresen, 2004), and grain boundary wetting by fluids (Rybacki and Dresen, 2000, 2004; Tullis et al., 1996) and melts (Tullis and Yund, 1992; Ji, 1987; Dell' Angelo et al., 1987; Mancktelow and Pennacchioni, 2004) favor grain boundary controlled diffusion creep over dislocation creep. Barring Stűnitz et al. (2003) who used millimeter-sized cores of single crystal plagioclase grains, most experiments on plagioclase deformation are conducted with aggregates of grains typically smaller than 200 μm. These experiments, therefore, do not replicate diffusion to dislocation creep switchover for coarser-then-experiment plagioclase grains in natural settings.

Understanding high-temperature deformation mechanisms in plagioclase in natural settings require rocks to be deformed at near-solidus condition (Tullis, 1983; Paterson et al., 1989;

* Corresponding author.
E-mail addresses: abbhat55@yahoo.com, abba@gg.iitkgp.ernet.in (A. Bhattacharya).

0191-8141/$ - see front matter © 2007 Elsevier Ltd. All rights reserved.
doi:10.1016/j.jsg.2007.04.005

Paterson and Fowler, 1993; Park and Means, 1996; Vernon et al., 1983, 1988, 2004). In the past, such studies were largely restricted to felsic intrusives (Fitzgerald and Stunitz, 1993; Rosenberg and Riller, 2000; Rosenberg and Stűnitz, 2003; Vernon et al., 2004), and only a few examples relate to anorthosites (Kruse et al., 2001; Lafrance et al., 1996). Between the two varieties, anorthosites are better suited to understand high-temperature deformation behavior of plagioclase because of two reasons. First, the solidus of gabbro-anorthosites at $T \geq 950\ °C$ (Green, 1966; Fram and Longhi, 1992) is substantially higher compared to that of felsic melts. Second, felsic intrusives contain modest proportion of quartz and micas. Therefore, deformation in felsic rocks is to a large extent accommodated by micaceous minerals generally weak to shear, and by ductile flow of quartz. In anorthosite, however, these mineral are rare or occur in accessory amounts, and therefore, the partitioning of bulk strain is likely to be small.

A wide variety of hitherto unreported plagioclase microstructures is documented from the Bolangir anorthosite pluton (Orissa, India) emplaced synchronous with regional deformation. The microstructures in larger-than-experiment plagioclase grains (200–2500 μm) indicate a switch form dislocation creep in the pluton interior to melt-assisted grain boundary controlled diffusion creep in the pluton margin.

2. Background geology

The Bolangir anorthosite pluton (~430 sq. km; Fig. 1) in the Eastern Ghats Mobile Belt of India is dominated by anorthosite; leuconorite and ultramafic pods occur in subordinate proportions (Mukherjee, 1989; Mukherjee et al., 1986, 1999; Bhattacharya et al., 1998). The anorthosites are characterized by bi-modal size population of plagioclase grains (Fig. 2a), with coarse plagioclase grains (up to ~14 cm long) of magmatic origin embedded in a fine-grained (<1 mm) mosaic of recrystallized plagioclase that replace former magmatic grains. The size and frequency of occurrence of the magmatic grains decrease towards the pluton margin (Fig. 2b). Anorthosites in the pluton interior are devoid of planar or linear fabrics, and often preserve relict cumulus texture (Fig. 2a). Towards the margin, an outward dipping margin parallel foliation is increasingly perceptible in anorthosites (Fig. 2b). The fabric is defined by bi-mineralic aggregates of recrystallized plagioclase and orthopyroxene grains (rarely ilmenite) or the preferred alignment of biotite flakes.

The pluton is separated from the enveloping granulites by blastoporphyritic K-feldspar bearing granitoids (Fig. 1). The earliest tectonic fabric in the granitoids at the contact with the pluton is invariably parallel to the foliation in anorthosites. The fabric is asymmetrically folded, with the gently plunging fold axes parallel to the massif-granitoid contact. Distal from the contact, the fabric in the granitoid weakens, and folds are notably absent. In the enveloping granulite facies gneisses, the WSW-ENE gneissic fabric in zones distal from the pluton is near orthogonal to the western margin of the pluton (Fig. 1). In zones (<4 km wide) neighboring the pluton margin (Fig. 1), the fabric in enveloping granulites is deflected parallel to the intrusives (cf. Reesor, 1958; Buddington, 1959; Paterson and Fowler, 1993). High strain necessary for ductile wall rock flow around non-piercing plutons prevail for distances >1 body radius of the pluton (Paterson and Fowler, 1993). In the Bolangir pluton, the width of aureole is significantly smaller compared to the body radius (~10 km). This coupled with the reoriented structures in the aureole suggest the anorthosite body at Bolangir was a "piercing" pluton emplaced discordant to the existing structures (Fig. 1).

Ferrodiorites along the margin of the pluton are Fe-rich (FeO ~35 wt%) melts unusually enriched in plagioclase-incompatible elements (P_2O_5 ~2.93 wt%; Zr ~5600 ppm; LREEs ~1200 times chondrite abundance), and characterized by negative Eu anomalies (Raith et al., 1997; Bhattacharya et al., 1998). The ferrodiorites inferred to be residual melts of anorthosite crystallization (Bhattacharya et al., 1998) occur as pods and sheets conformable with the pluton margin parallel foliation in anorthosites. Ferrodiorites are also emplaced along N-S trending ductile shear zones oblique to the margin-parallel foliation in anorthosite (Fig. 2c,d). The occurrence of ferrodiorites concordant with and discordant to the margin-parallel foliation suggests a close temporal relationship between regional stress and the presence of melts during pluton deformation.

2.1. P-T conditions

Compositions of texturally identified magmatic plagioclase in anorthosites are tightly constrained between An_{52} and An_{59} (Fig. 3a). The plagioclase grains are weakly zoned to An-richer compositions, but the chemical variations generally do not exceed 2 mol% An. Plagioclases richer in anorthite component (An_{70} and An_{85}) correspond to two textural types. Plagioclase (An_{60-85}) intergrown with vermicular orthopyroxene formed by sub-solidus decomposition of garnet (Prasad et al., 2005). The other set of plagioclase compositions (An_{69-72}) are restricted to anorthosites neighboring the pluton margin, but are absent in the more centrally located parts of the pluton. The An-richer compositions constitute <100 μm wide rims along margins of An-poorer recrystallized plagioclase grains separated by K-feldspar films (Fig. 3b). Similar reverse zoning in magmatic plagioclase in anorthosites (Emslie, 1980; Dymek, 1981; Morse and Nolan, 1984) were interpreted to suggest crystallization from melts along grain boundaries (Emslie, 1980) or inter-granular melts super-saturated in the An component (Morse and Nolan, 1984).

Fram and Longhi (1992) experimentally determined the effect of pressure on the liquidus phase relations in high-Al gabbroic melts. The magmatic plagioclases (An_{52}–An_{56}) in the Bolangir anorthosites chemically overlap with the liquidus plagioclase An_{54-60} in Fram and Longhi's (1992) experiments at $P > 7$–12 Kbar for $T > 1000\ °C$ (Fig. 3a). The metamorphic P-T estimates are, however lower, e.g. 600–700 °C and 5–6 kbar (Mukherjee et al., 1986, 1999). Prasad et al. (2005; sample L-19; location in Fig. 1), computed the metamorphic P-T conditions for garnet breakdown

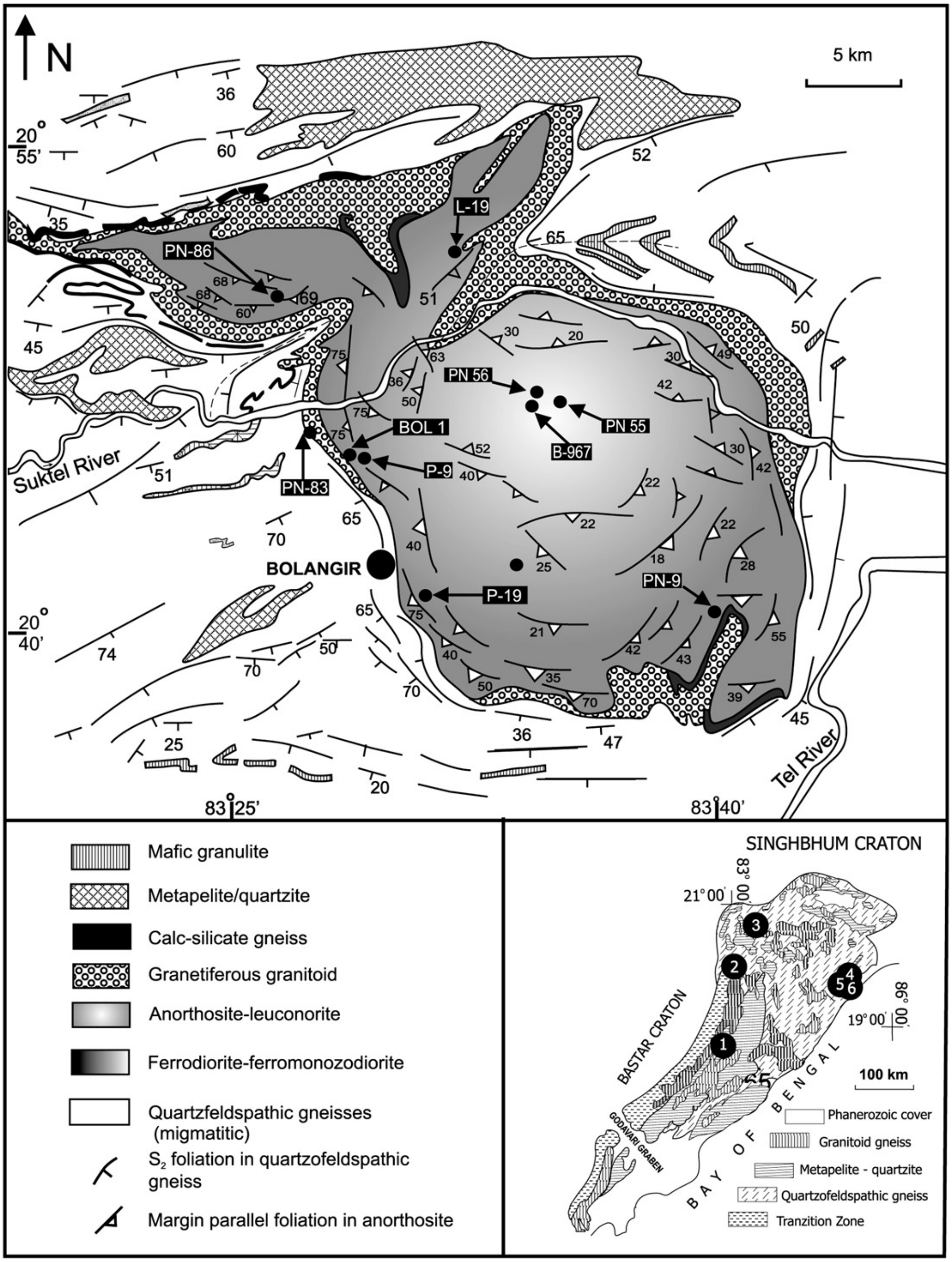

Fig. 1. Key lithological units and dominant structural trends within the anorthosite pluton at Bolangir and the bordering granulite gneisses (modified after Bhattacharya et al., 1998). The foliation in granulite gneisses S_2 is axial planar to isoclinal folds on the earliest planar fabric S_1. The gneissic fabric in granitoids bordering the pluton is parallel to the pluton margin. Filled boxes are location numbers of samples cited in text. Inset shows the locations of anorthosite plutons in the Eastern Ghats Belt (modified after Ramakrishnan et al., 1998; Leelanandam and Reddy, 1988), e.g. 1 − Koraput, 2 − Turkel, 3 − Bolangir, 4 − Banpur/Balugaon, 5 − Rambha, 6 − Kalikota.

to orthopyroxene + An-rich plagioclase to be $750 \pm 50\,^{\circ}C$ and 6 ± 1 kbar. The P and T of pluton emplacement are bracketed by the two sets of P-T estimates. However, the emplacement P-T condition is likely to be closer to the magmatic P-T estimate, in view of the presence of ferrodiorite melts during pluton emplacement.

3. Microstructure

3.1. Analytical techniques

Transmitted light microscopy was done on 2 cm × 5 cm and 5 cm × 7.5 cm sized thin sections of more than 80

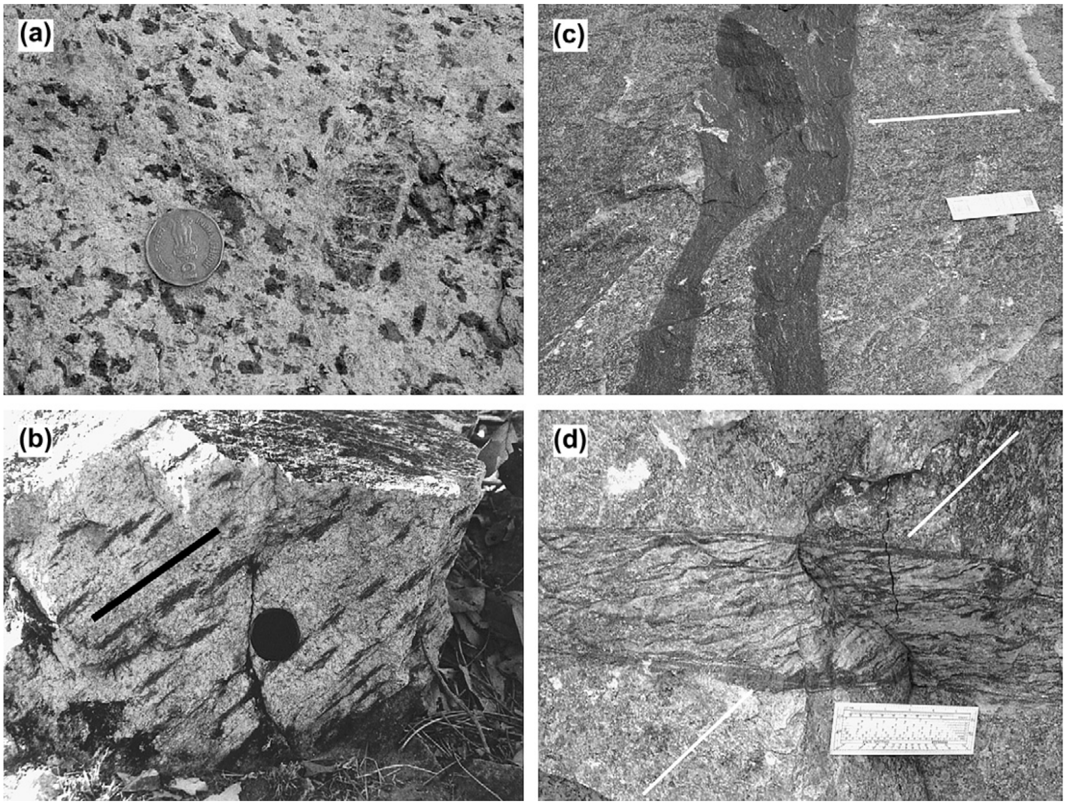

Fig. 2. Field features. (a) Anorthosite (PN-56) in the pluton interior showing the lack of planar fabric, and the bimodal size population among plagioclase grains, e.g. grey colored magmatic grains in finer-grained recrystallized mosaic. Coin diameter = 2.5 cm. (b) Margin parallel foliation (parallel to the thick black line) in anorthosites defined by bi-phase lenticular aggregates of biotite and plagioclase. Note the absence of gray colored plagioclase grains. Lens cap diameter = 5 cm. (c) Ferrodiorite dykes (PN 9) discordant to the pluton-margin parallel foliation (white line) in anorthosite. (d) Ferrodiorite (PN 9) residual melts emplaced along both S and C fabrics oblique to margin-parallel foliation in anorthosite.

anorthosites. Morphometric analyses of plagioclase grains (Fig. 4) are presented for 4 representative samples along an E-W traverse, two each from the margin and the interior of the pluton. The samples from the pluton margin were cut in two directions, one set orthogonal to the margin-parallel foliation, and the other parallel to the foliation. Since planar or linear fabrics in anorthosites in the pluton interior were lacking, thin sections were prepared along two arbitrarily-chosen mutually-orthogonal directions. For each sample, grain intercept (Vander-Voort and Gokhale, 1992; Fig. 4a) of plagioclase were measured on traced grain boundaries of crossed polar images in a tracing sheet using the ImageJ software (http://rsb.info.nih.gov/ij). The digitized boundaries of plagioclase grains were fitted by equivalent area ellipses using the "fitellipse" macro in the ImageJ software. The angles subtended by major axes of ellipses to a fixed horizontal axis were measured. The angles were plotted in circular frequency diagrams (Fig. 4b) to determine the preferred alignment among plagioclase grains.

3.2. The pluton interior

The coarser plagioclase grains (typically >3 mm; largest ~14 cm long) are inequant, internally-strained (kinked cleavage, strain wavy extinction, bent twins, spindle-shaped deformation twins, and bulge nucleation; Fig. 5a,b), and characterized by high-energy grain boundaries (Fig. 5c). The finer-sized plagioclase grains (intercept length 200–600 μm; Fig. 4a) are equant to sub-equant, internally-strained, and characterized by high energy grain boundaries (Fig. 5b,d), although well-equilibrated boundaries are locally present. Magmatic flow texture (Den Tex, 1969) is not obvious in anorthosites. In a rare instance, tiled grains of euhedral plagioclase enclosed within a large orthopyroxene grain were observed (Fig. 5e). The orthopyroxene oikocrysts are not internally strained (Fig. 5a). The finer-grained plagioclase grains are continuous with and anchored to the recrystallized plagioclase aggregates in healed micro-cracks within former magmatic plagioclase grains. The compositions of the finer-grained plagioclase aggregates and the former magmatic grains chemically overlap (Fig. 5d). This implies that the finer-sized plagioclase grains were not products of magmatic crystallization, and instead replaced magmatic plagioclase by grain boundary migration recrystallization accommodated dislocation creep (cf. Vernon et al., 2004). Although deformation-recrystallization seemingly outlasted solidification of melts, the healed microcracks in the magmatic grains appear to be facilitated by small gradients in plastic strain energy in plagioclases weakened by the presence of small amounts of melts (cf. Cooper and Kohlstedt, 1984; Dell' Angelo et al., 1987; Vernon et al., 2004) or fluids

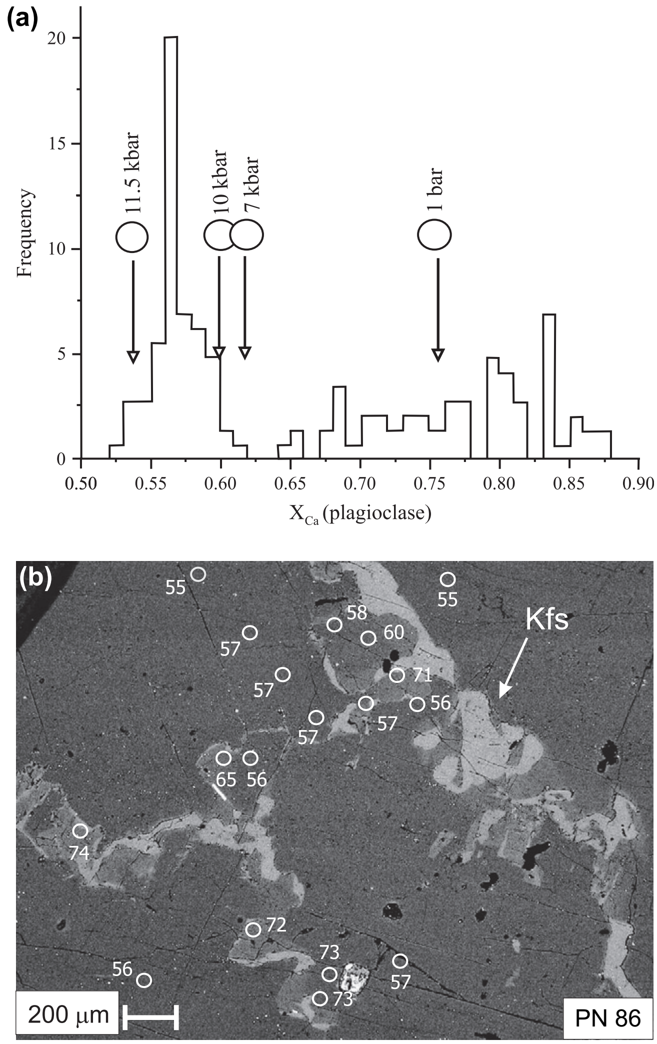

Fig. 3. (a) Variations in An mol % in plagioclase from anorthosite in the Bolangir pluton. Unfilled circles with numbers are the composition of liquidus plagioclase determined by Fram and Longhi (1992) at the pressure indicated alongside. (b) BSE image showing compositional variations in recrystallized plagioclase grains in anorthosite from the pluton margin. The plagioclase grains show core-to-rim weak reverse zoning (An_{55-57}). Anorthite content along grain boundaries (lighter tones neighboring K-feldspar grains) increases to An_{69-72}.

(cf. Urai et al., 1986). Ductile deformation in plagioclase is initiated at ~450 °C (Tullis and Yund, 1991; McLaren and Pryer, 2001; Stűnitz et al., 2003), and that of orthopyroxene ≥800 °C (Gil Ibarguchi et al., 1999). Apparently, deformation of the pluton interior occurred at temperature limited by the two sets of values, but closer to the higher estimate because of the likely presence of small volume of melt.

3.3. The pluton margin

The margin parallel foliation in anorthosites is defined by bi-mineralic aggregates of polygonal plagioclase grains (max intercept length <200 μm) and strain-free grains of orthopyroxene or shape preferred biotite flakes. Beyond the aggregates, kink bands, bent cleavages and strain wavy extinction provide evidence of internal lattice strain in magmatic orthopyroxene grains (Fig. 6a).

Compared to the pluton interior, plagioclase in anorthosites from the pluton margin are coarser and poly-sized (Fig. 4a), characterized by wide dispersal of dihedral angles, and show prominent shape preferred alignment (Fig. 4b). Plagioclase grains are classified into two textural groups. Group 1 plagioclase grains are coarse (>½ mm long), rectangular (Fig. 6b) rather than polygonal, and with poorly-developed rational faces. The plagioclase grains are strain-free, but characterized by weak undulose extinction near the bulged grain boundaries. Impingement between neighboring rectangular shaped plagioclase grains is common (Fig. 6c), but strain effects neighboring the impingements cannot be resolved by microscopic examination. Vernon et al. (2004) explained grain impingement and associated truncated chemical zoning in plagioclase to indicate melting along grain contact. The interfaces between adjacent group 1 plagioclase grains are occasionally laced by K-feldspar films (Figs. 3b and 6d). A total of <100 μm wide zones along plagioclase margins adjacent to the K-feldspar films are chemically zoned to more An-richer composition, e.g. An_{68-72} (Fig. 3b) The An-richer plagioclase margins, often "spear-shaped" or rectangular (Fig. 6d) in appearance, indent into adjacent group 1 plagioclase grains. Strain effects neighboring the indentations are not evident.

Group 2 plagioclase grains, comparable in size to and intimately associated with group 1 plagioclase, are euhedral, chemically unzoned, strain-free and un-recrystallized. End-to-end touching plagioclase grains locally constitute linear trails, and show grain tiling (Fig. 7a). Microstructural criteria for identifying magmatic flow in plutonic rocks have been discussed by several authors (Den Tex, 1969; Nicolas, 1992; Nicolas and Ildefonse, 1996; Higgins, 1998; Paterson et al., 1989; Sawyer, 2001; Vernon, 2004). The consensus emerging from these views is that magmatic flow is best manifested by the parallel alignment of touching euhedral plagioclase grains, in the absence of plastic deformation in or recrystallization of the aligned crystals, and are unbroken (Paterson et al., 1989). Vernon et al. (2004) suggests that albite twin planes should necessarily be parallel to the long dimension of the plagioclase grains. Imbrication or tilling of euhedral grains (Den Tex, 1969) has also been suggested to indicate non-coaxial magmatic flow (Paterson et al., 1989; Nicolas and Ildefonse, 1996; Sawyer, 2001; Vernon, 2004). The criteria above are largely met by the textures (Fig. 7a) of group 2 plagioclase grains. The thin films of An-richer margins of group 1 plagioclase cannot be recrystallized equivalents of An-poorer interiors of the plagioclase grains. Instead the An-richer rims in group 1 plagioclases may constitute, in all likelihood, overgrowths crystallized from intergranular melts (cf. Dell' Angelo et al., 1987; Fig. 4, Tullis and Yund, 1991; Rosenberg, 2001; Marchildon and Brown, 2002).

Based on experimental studies, Tullis and Yund (1991) suggest the following features in plagioclase grains to indicate deformation by diffusion creep, e.g. grains with rectangular outlines and low dislocation density, existence of pores/channels along grain boundaries and overgrowths chemically different from larger grains. Truncation of zoning by indenting grains and fine-scale dissolution were suggested to indicate diffusion creep by Gower and Simpson (1992). Garlick and Gromet (2004) inferred mixed phase distribution, high-energy lobate/cuspate phase boundaries and predominance of equant to sub-equant grains with low internal strain to be manifestations of melt-enhanced diffusion creep.

The following microstructures in group 1 plagioclase suggest deformation by grain boundary controlled diffusion creep: (a) the predominance of rectangular-shaped grains with low or no internal strain that share high-energy boundaries widely dispersed about 120°; (b) indenting nature of anorthite-richer overgrowths on weakly zoned grains into neighboring plagioclase; and (c) impinged grains that truncate zoning profiles, yet did not produce visible strain in the indented grain neighboring the piercement. Grain boundary sliding (Rosenberg and Handy, 2000) is possibly a necessary consequence of deformation by diffusion creep (Poirier, 1985; Garlick and Gromet, 2004). Grain shape changes induced by diffusion creep result in incoherent grain contact (open spaces) and that are accommodated by grain boundary sliding (Adams and Murray, 1962; Langdon and Vastava, 1982; Poirier, 1985; Gower and Simpson, 1992; Lapworth et al., 2002; Rosenberg and Stűnitz, 2003; Garlick and Gromet, 2004). The best evidence of grain boundary sliding in the marginal zone of the Bolangir anorthosite pluton is provided by the varying lattice orientation (alignment of basal cleavage) of biotite grains along the margins of plagioclases (Fig. 7b,c). Similar textures involving amphiboles were invoked by Garlick and Gromet (2004) and Kruse and Stunitz (1999) in favor of grain boundary sliding. The occurrence of strain-free rectangular plagioclase grains with straight grain boundaries against biotite flakes (Fig. 7d) is also inferred to indicate melt-assisted grain boundary sliding during diffusion creep.

3.4. Spatial variation in plagioclase deformation mechanisms

In contrast to the intercept lengths of recrystallized plagioclase grains (~100–600 μm) in the pluton interior, the majority of multi-sized plagioclase grains (200–2500 μm) in the pluton margin are larger (Fig. 4a). Since strain rates are inversely related to the cube of grain size (Poirier, 1985), the dominance of grain boundary controlled diffusion creep (Cobble creep), in preference to dislocation creep, in coarser grained rocks (Rybacki and Dresen, 2004) is a major concern. The presence of melts is known to promote diffusion creep (Kohlstedt and Zimmerman, 1996; Tullis et al., 1996; Hirth and Kohlstedt, 2003) in multigrain aggregates and synthetic analogues. The anorthosite-residual melts concordant with

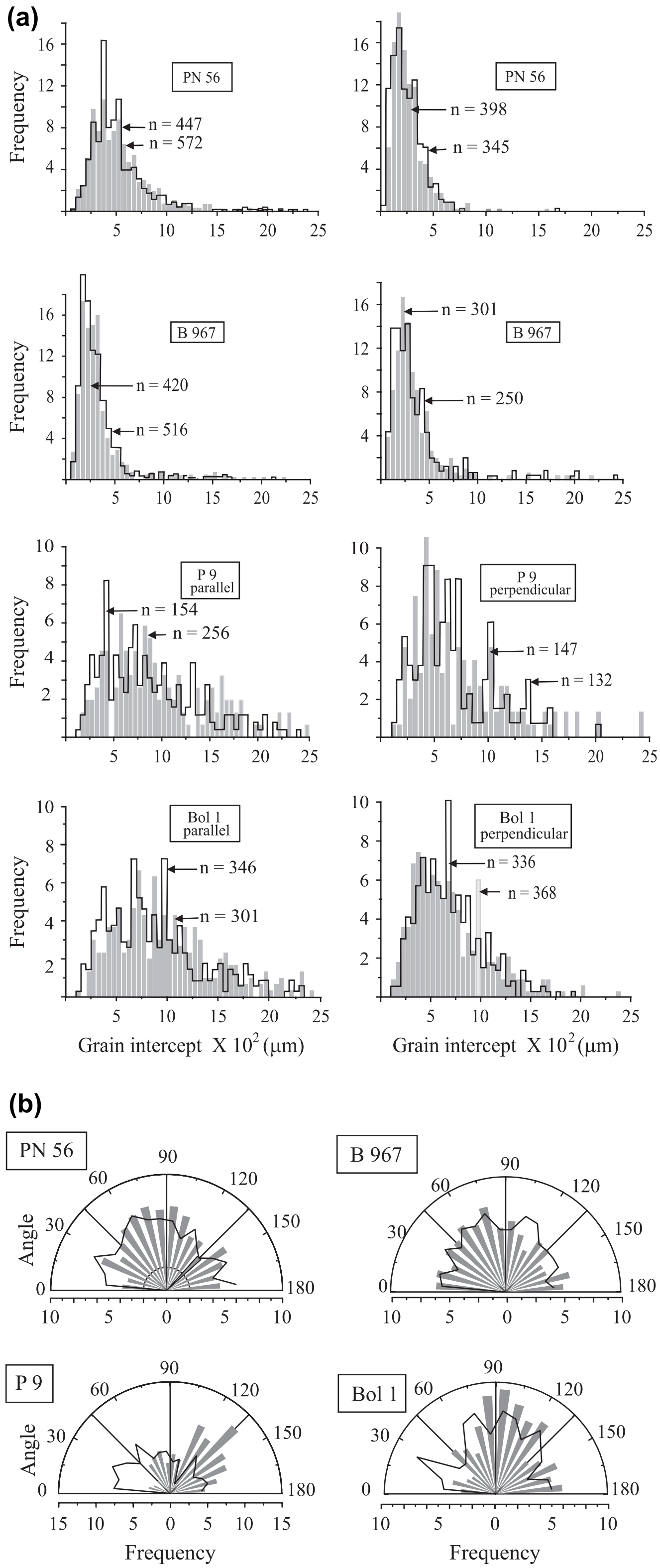

Fig. 4. Results of morphometric determinations of plagioclase in anorthosites. (a) Frequency plots of grain intercepts (in μm) in anorthosites from the pluton interior (PN 56, B967) and the pluton margin (Bol 1, P 9). The frequency plots (in gray shades and by continuous lines) correspond to two orthogonal directions (see text for details). In samples from the pluton margin, "parallel" and "perpendicular" refer to orientations of sections relative to the margin-parallel foliation. For samples from the pluton interior, grain intercepts >600 μm correspond to relict magmatic grains. "*n*" refers to the number of grains in which intercepts were measured. (b) Circular frequency plots of preferred orientation of plagioclase grains from the pluton interior (top set) and the pluton margin (bottom set) relative to an arbitrarily chosen reference line that coincides with 0° in the circular plot. In the bottom set diagrams, the frequency plots in gray shades and by continuous lines correspond to sections parallel and perpendicular respectively to the margin-parallel foliation.

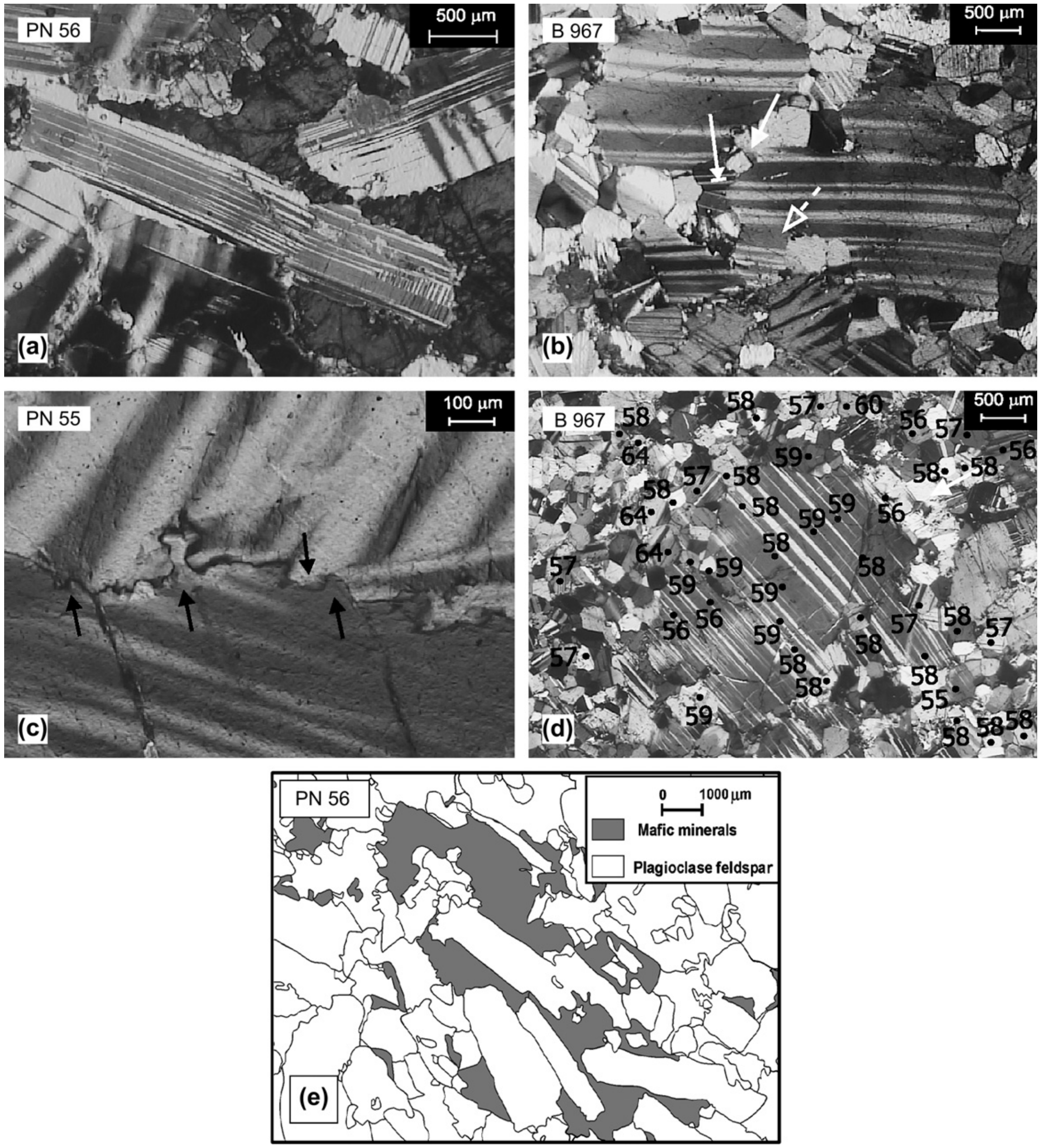

Fig. 5. Crossed polar images (barring line sketch in e) of plagioclase microstructures in pluton-interior anorthosites. (a) Deformation bands in magmatic plagioclase grains, but magmatic orthopyroxene grains are not internally strained. Plagioclase margins are bulged against orthopyroxene. (b) Deformation twins in former magmatic grains are displaced relative to each other adjacent to microfracture (subsequently healed). Bulge nucleation (arrow) and the neo-crystallized grains (arrowhead with bar) within deformation twins are shown. Sub-grains (unfilled broken arrow) are common proximal to the healed microfractures. The recrystallized grains along the microfracture are continuous with and anchored to recrystallized grains bordering the fragmented magmatic grain. (c) Serrated margin and grain boundary bulges between adjacent magmatic plagioclase grains. (d) A magmatic plagioclase grain (centre) occurring as raft within finer-sized plagioclase grains. Anorthite content in plagioclase (mol %) grains indicated against the analyzed spots (filled circles). The finer-sized plagioclase grains are characterized by un-equilibrated grain boundaries. (e) Line sketch showing grain tilling among euhedral plagioclase grains enclosed in coarse orthopyroxene. The structure occurs as a raft within recrystallized plagioclase grains.

and discordant to margin-parallel foliation, magmatic flow texture among euhedral plagioclase grains flow (cf. Guineberteau and Vigneresse, 1987; Vernon et al., 1988; Paterson et al., 1989) and indenting overgrowths of anorthite-richer plagioclase indicate the presence of melts during pluton deformation in the marginal zones. In all probability, a combination of syn-deformational melts and enhanced strain rates due to melts (cf. Jin et al., 1994; Hirth and Kohlstedt, 1995) facilitated grain boundary controlled diffusion creep in plagioclase along the pluton margin.

In contrast to the inferred presence of small melt fraction in the pluton interior, the ability of plagioclase crystals (group 2) to rotate and align along flow layers indicates larger melt fraction existed during deformation of the pluton margin. The presence of variable proportion of melt in the pluton suggests that the temperature during deformation of the pluton interior

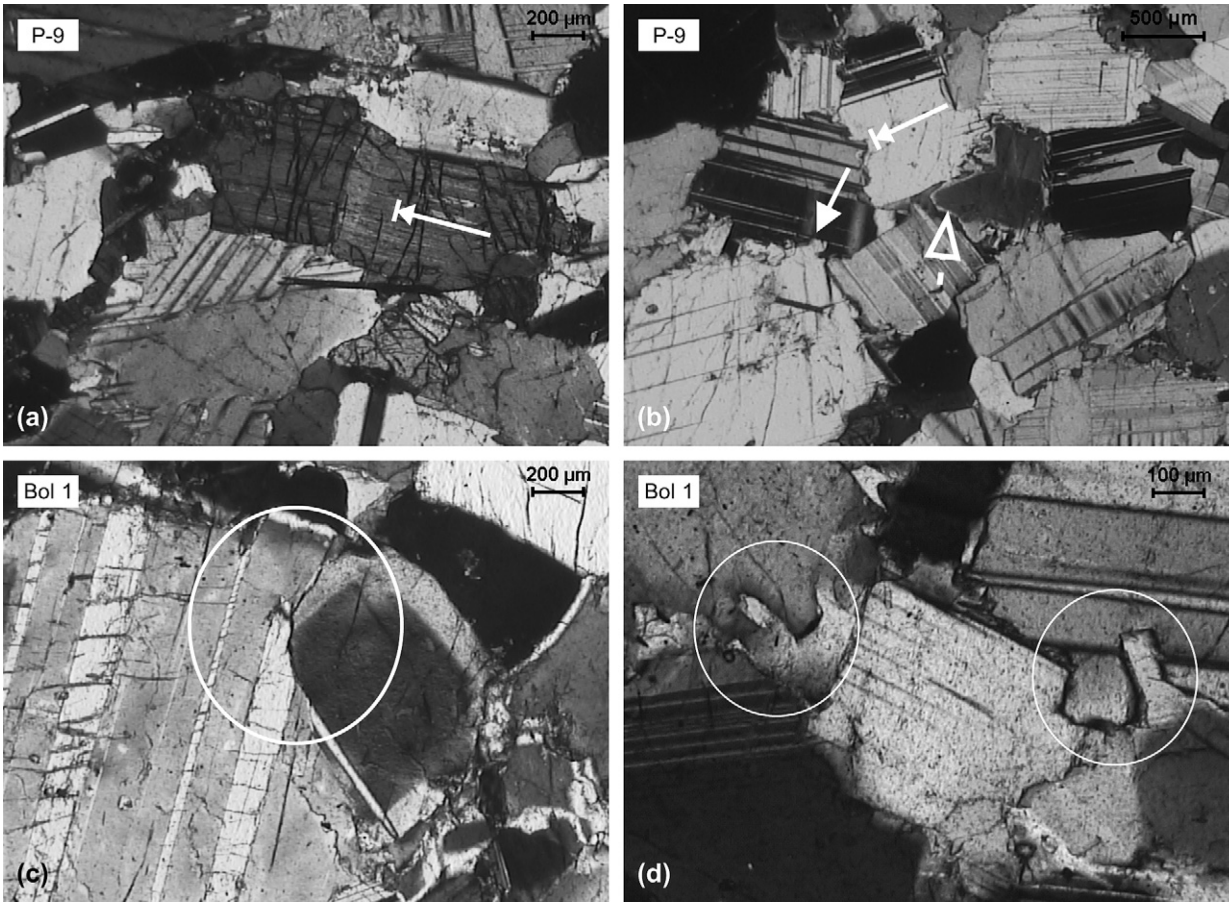

Fig. 6. Crossed polar images of plagioclase microstructures in pluton-margin anorthosites. (a) Deformation twins in magmatic orthopyroxene grains (arrowhead with bar). Pinned plagioclase grains against the orthopyroxene grain are absent. (b) Rectangular plagioclase grains (group 1) showing shape preferred alignment. Grain boundary bulges (filled arrow) and serrated grain boundaries (arrow with bar) indicated. K-feldspar films between high-anorthite grain boundaries of adjacent plagioclase grains shown by unfilled broken arrow. (c) Grain impingement (within circle) among rectangular plagioclase grains. The chemical zoning in the plagioclase grain (right-centre) is truncated. (d) Group 1 plagioclase grains indenting (circles) neighboring plagioclase grains. The group 1 plagioclase grains adjacent to the indentation lack strain and are zoned to anorthite-richer composition.

was comparable throughout pluton. Therefore, temperature gradient within the pluton alone could not have induced the interior to margin switch in deformation mechanisms in plagioclase. Instead, the switch in plagioclase deformation processes must have been induced by the varying fraction of melt (crystal/melt ratio), i.e. higher at the margin compared to the interior.

4. Pluton deformation

A convenient starting point for understanding pluton deformation during emplacement is to consider the pluton comprising grain-supported resident melts was emplaced in a regionally deforming crust. Deformation of the pluton was effected by two opposing stress fields, i.e. pluton expansion due to magmatic flow acting from interior to the margin (Paterson et al., 1998; Paterson and Fowler, 1993), and the far field stress (east-west shortening) acting inwards into the pluton. Therefore, deformation at the pluton margin may be likened to the development of a high temperature shear zone.

Since melts decrease the viscosity of deforming medium (Barraud et al., 2004), partitioning of bulk strain was inescapable within the pluton depending the volume fraction of melt present at any instant of time. Melt-richer parts accommodated the shearing component of the bulk strain manifested by non-coaxial magmatic flow. But melt-poor parts comprising touching grains experienced progressive shortening and deformation. In view of the time-space instability of a heterogeneous crystal-melt mush of a deforming pluton, a large variety of microstructures operated in varying scales in different parts of the pluton. In domains that started with high resident melt fractions, non-coaxial magmatic flow led to grain tilling (cf. Nicolas, 1992). Deformation driven melt expulsion from these domains, led to grain to grain contact, and the melt-wetted plagioclase grains experienced grain boundary sliding in response to the imposed stress, thus largely preserving the rectangular grain shapes. Biotite grains along the plagioclase grain boundaries aided grain boundary sliding (cf. Hirth and Kohlstedt, 1995; Park and Means, 1997). With continued porosity destruction and melt expulsion, the touching plagioclase grains were deformed by melt-enhanced grain

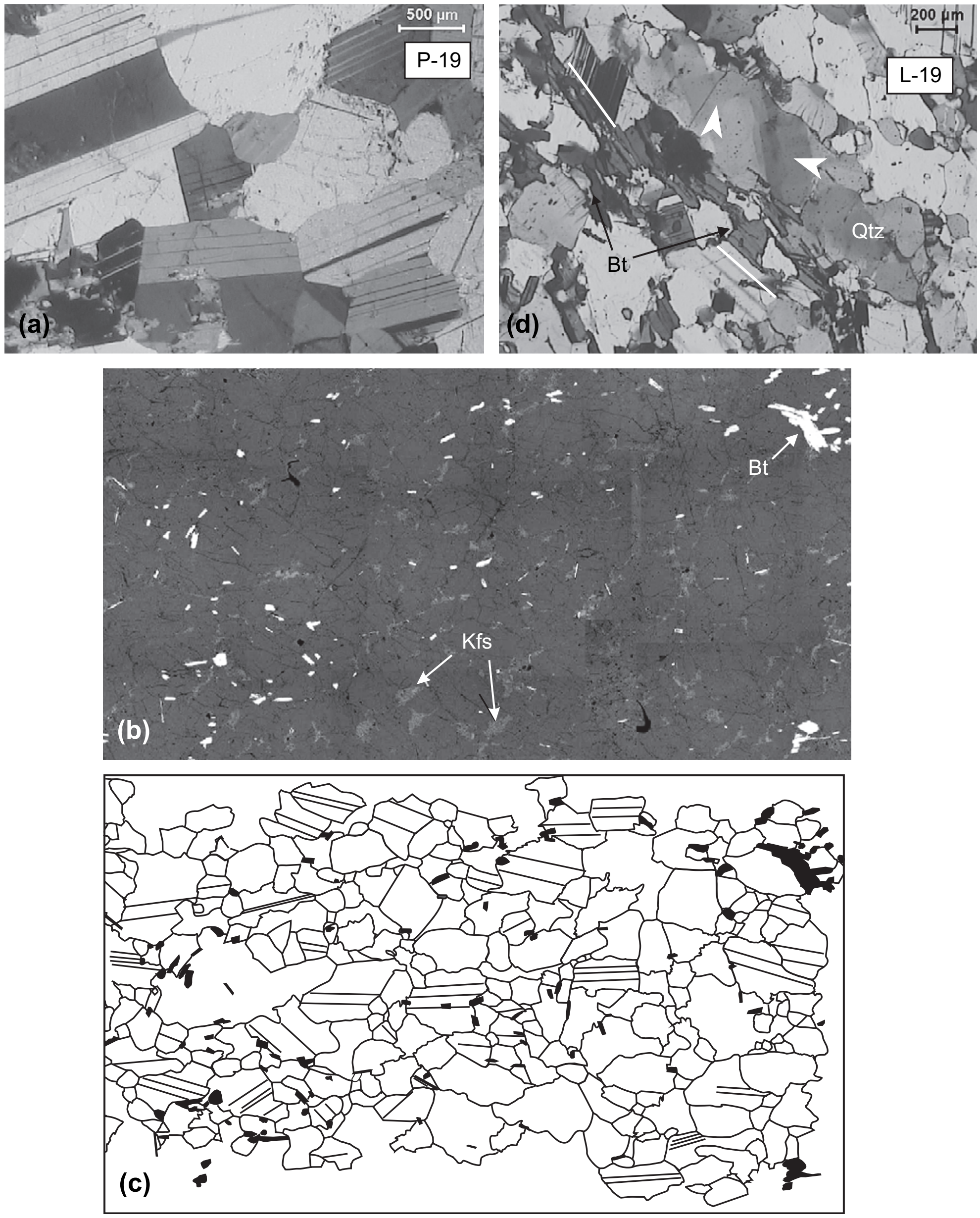

Fig. 7. Microstructures in anorthosites from the pluton margin. (a) End-to-end touching and side-to-side tiled grains of group 2 (magmatic) plagioclase grains (image in crossed polars; P-19). The margins of the unstrained euhedral magmatic plagioclase grains are only marginally modified by recrystallization. (b) BSE and (c) line sketch of the same field of view in P 19. In the line sketch, outlines of euhedral/subhedral group 2 plagioclase grains are shown, and albite twin orientations in the grains are indicated by parallel lines. Note the weak preferred alignment among magmatic plagioclases (left to right). Biotite flakes lodged along plagioclase margins are variably oriented. A majority of biotite (Bt) flakes and K-feldspar (Kfs) films (cf. Fig. 3b) along plagioclase grain boundaries occur parallel to each other (left-bottom to right-top), and sub-parallel with the alignment of group 2 plagioclase grains. (d) Relatively strain-free rectangular grains of plagioclase with boundaries limited by the basal cleavages of biotites (filled arrows) in anorthosite sample L 19. Plagioclase grains in the biotite-plagioclase bi-phase aggregates are smaller and pinned. The quartz (Qtz) lenticle showing chessboard twinning (unfilled arrows) is parallel to the biotite flakes.

boundary sliding (Hirth and Kohlstedt, 1995; Park and Means, 1997) accommodated diffusion creep at the high temperature and prevalent strain rates. This possibly explains the close association of the magmatic flow textures (group 2 plagioclase) and diffusion creep textures (group 1 plagioclase) in anorthosites at the pluton margin. On the contrary, microtextural features in the pluton interior indicate deformation-recrystallization to have largely outlasted magmatic flow/expansion of the pluton, although microstructural features seem to suggest small amounts of melts resided along grain boundaries.

If the pluton margin is analogous to a shear zone, one needs to explain the coarser sizes of plagioclase grains along the pluton margin relative to the interior. It is important to recall that size reduction of plagioclase in the pluton interior via grain boundary accommodated dislocation creep largely post-dated growth of plagioclase by magmatic crystallization. By contrast, deformation in the pluton margin was achieved in the presence of larger volume fraction of melt (enabling plagioclase grains to rotate by non-coaxial magmatic flow). By implication, the magmatic plagioclase grains (group 2) continued to grow and coarsen in the magmatic state during deformation, unlike in the pluton interior where former magmatic plagioclases experienced size reduction. Further, a majority of group 1 plagioclase grains in the pluton margin may essentially represent group 2 magmatic grains that subsequently experienced grain growth by melt-assisted diffusion creep. Another mechanism that may account for the larger size of recrystallized plagioclase grains along the pluton margin is analogous to strain-enhanced grain growth. Void spaces produced by diffusion creep and grain boundary sliding may also be healed by grain boundary migration sweeping across the voids (Wilkinson and Caceres, 1984). Since shear stresses during pluton emplacement were arguably among the highest neighboring the pluton margin, grain boundary sliding at the prevailing high strain and strain rate may lead to crumpling of grain boundaries increasing the surface area of the grains (cf. Wilkinson and Caceres, 1984). Grain boundary migration in tandem with diffusion creep may have contributed to deformation enhanced grain growth in plagioclase near the pluton margin. In comparison, the magnitude of strain experienced by the deforming pluton interior was arguably lower, thereby inhibiting enhanced grain growth.

5. Conclusions

The inferences made in this study are the following: (1) ferrodiorites (residual melts of anorthosite crystallization) parallel to and discordant with the pluton-margin parallel foliation, magmatic flow among euhedral plagioclase grains in domains neighboring the pluton margin, and thermo-barometric estimates attest to near-solidus high temperature deformation of the pluton; (2) the pluton interior experienced grain boundary migration recrystallization accommodated dislocation creep initiated along dissection microstructures in magmatic plagioclase grains weakened by the presence of small amounts of melt; (3) the margin-parallel foliation in anorthosites defined by the preferred alignment among magmatic plagioclase (group 2) and lenticles of recrystallized bi-mineralic aggregates is attributed to magmaric flow and solid state deformation during syn-deformational emplacement of the pluton; and (4) in the pluton margin, poly-sized, largely-unstrained and rectangular-shaped plagioclase grains with high-energy An-richer boundaries indenting and impinging into neighboring plagioclase grains are inferred to indicate plagioclase (group 1) deformation by grain boundary migration accommodated diffusion creep during sub-magmatic flow. The margin-to-interior variation in plagioclase deformation microstructures is correlated with decrease in melt/crystal ratio consistent with experimental studies and numerical models that demonstrate melts to promote diffusion creep in plagioclase at high temperature. The significance of this study is that the inference is true when extended to significantly coarser-than-experiment plagioclase grains.

Acknowledgments

PN acknowledges the financial support from the University Grants Commission (India) to carry out the research work in connection with his doctoral dissertation. J.A. Tullis and M. Higgins provided relevant literature on the subject at short notice. AB acknowledges the financial support provided by the PLANEX program (Physical Research Laboratory, Ahmedabad, India) for carrying out a part of the work. The journal reviewers M. Egydio-Silva and H. Stunitz provided comments and suggestion on the manuscript that helped to focus out thoughts. The scientific content and style of presentation of the manuscript greatly befitted from these reviews.

References

Adams, M.A., Murray, G.T., 1962. Direct observations of grain boundary sliding in bi-crystals of sodium chloride and magnesia. Journal of Applied Physics 33, 2126–2131.

Barraud, J., Gardien, V., Allemand, P., Grandjean, P., 2004. Analogue models of melt-flow networks in folding migmatites. Journal of Structural Geology 26, 307–324.

Bhattacharya, A., Raith, M., Hoernes, S., Banerjee, D., 1998. Geochemical evolution of the massif-type anorthosite complex at Bolangir in the Eastern Ghats Belt of India. Journal of Petrology 39, 1169–1195.

Buddington, A.F., 1959. Granite emplacement with special reference to North America. Geological Society of America Bulletin 70, 671–747.

Cooper, R.F., Kohlstedt, D.L., 1984. Solution-precipitation enhanced diffusion creep of partially molten olivine-basalt aggregates during hot-pressing. Tectonophysics 107, 207–233.

Den Tex, E., 1969. Origin of ultramafic rocks, their tectonic settings and history: a contribution to the discussion of the paper: "The origin of ultramafic and ultrabasic rocks" by PJ Wyllie. Tectonophysics 7, 457–488.

Dell' Angelo, L.N., Tullis, J., Yund, R.A., 1987. Transition from dislocation creep to melt-enhanced diffusion creep in fine-grained granitic aggregates. Tectonophysics 139, 325–332.

Dimanov, A., Dresen, G., Wirth, R., 1998. High-temperature creep of partially molten plagioclase aggregates. Journal of Geophysical Research 103, 9651–9664.

Dimanov, A., Dresen, G., Xiao, X., Wirth, R., 1999. Grain boundary diffusion creep of synthetic anorthite aggregates: the effect of water. Journal of Geophysical Research 104, 10483–10487.

Dimanov, A., Wirth, R., Dresen, G., 2000. The effect of melt distribution on the rheology of plagioclase rocks. Tectonophysics 328, 307–327.

Dymek, R.F., 1981. Reverse zoning in plagioclase from labradorite anorthosite, St. Urbain massif, Quebec: retrograde plag-pyx reaction? Geological Society of America Abstract Program 13, 444.

Emslie, R.F., 1980. Geology and petrology of the Harp Lake Complex, Central Labrador: an example of Elsonian magmatism. Geological Survey of Canada Bulletin 293, 1–136.

Fitzgerald, J.D., Stunitz, H., 1993. Deformation of granitoids at low metamorphic grade. I. Reactions and grain size reduction. Tectonophysics 221, 269–297.

Fram, M.S., Longhi, J., 1992. Phase equilibria of dikes associated with Proterozoic anorthosite complexes. American Mineralogist 77, 113–132.

Garlick, S.R., Gromet, L.P., 2004. Diffusion creep and partial melting in high temperature mylonitic gneisses, Hope Valley shear zone, New England Appalachians, USA. Journal of Metamorphic Geology 22, 45–62.

Gil Ibarguchi, J.I., Ábalos, B., Azcarraga, J., Puelles, P., 1999. Deformation, high-pressure metamorphism and exhumation of ultramafic rocks in a deep subduction/collision setting (Cabo Ortegal, NW Spain). Journal of Metamorphic Geology 17, 747–764.

Gower, R., Simpson, C., 1992. Phase boundary mobility in naturally deformed, high-grade quartzofeldspathic rocks: evidence for diffusional creep. Journal of Structural Geology 14, 301–313.

Green, P.H., 1966. High presuure experiments on the genesis of anorthosites. In: Petrology of the Upper Mantle. Publication No. 444, Department of Geophysics and Geochemistry, Australlian National University (Canberra), pp. 206–233.

Guineberteau, B., Vigneresse, J.-L., 1987. The Mortagne granite pluton (France) emplaced by pull-apart along a shear zone: structural and gravimetric arguments and regional implication. Geological Society of America Bulletin 99, 763–770.

Higgins, M.S., 1998. Origin of Anorthosite by textural coarsening: quantitative measurements of a natural sequence of textural development. Journal of Petrology 39, 1307–1323.

Hirth, G., Kohlstedt, D.L., 1995. Experimental constraints on the dynamics of the partially molten upper mantle: deformation in the diffusion creep regime. Journal of Geophysical Research 100, 1981–2001.

Hirth, G., Kohlstedt, D.L., 2003. Rheology of the upper mantle and the mantle wedge: a view from the experimentalists. In: Eiler, J. (Ed.), Inside the Subduction Factory. Geophysical Monograph, 138, pp. 83–105.

Huang, J., Dimanov, A., Wirth, R., Dresen, G., 2001. Diffusion creep of labradorite aggregates: effect of melt chemistry. AGU Transactions 82(47), F1144 (Fall Meeting 2001 Supplement).

Ji, S., 1987. Deformation plastique naturelle et experimentale des plagioclase. Ph.D. thesis, Univ. des Sci. et Tech. du Languedoc, Montpellier, France.

Jin, Z.M., Green, H.W., Zhou, Y., et al., 1994. Melt topology in partially molten mantle peridotite during ductile deformation. Nature 372, 164–167.

Kohlstedt, D.L., Zimmerman, M.E., 1996. Rheology of partially molten mantle rocks. Annual Review of Earth Planetary Sciences 24, 41–62.

Kruse, R., Stunitz, M., 1999. Deformation mechanisms and phase distribution in mafic high-temperature mylonites from Jotun Nappe, Southern Norway. Tectonophysics 303, 223–249.

Kruse, R., Stűnitz, H., Kunze, K., 2001. Dynamic recrystallisation processes in plagioclase porphyroclasts. Journal of Structural Geology 23, 1781–1802.

Lafrance, B., John, B.E., Scoates, J.E., 1996. Syn – emplacement recrystallisation and deformation microstructures in the Poe Mountain anorthosite. Wyoming. Contributions to Mineralogy and Petrology 122, 431–440.

Langdon, T.G., Vastava, R.B., 1982. An evaluation of deformation models for grain boundary sliding. In: Rohde, R.W., Swearengen, J.C. (Eds.), Mechanical Testing for Deformation Model Development. American Society for Testing materials, Philadelphia, pp. 435–451.

Lapworth, T., Wheeler, J., Prior, D.J., 2002. The deformation of plagioclase investigated using electron backscatter diffraction crystallographic preferred orientation data. Journal of Structural Geology 24, 387–399.

Leelanandam, C.K., Reddy, M.N., 1988. Precambrian anorthosites from Peninsular India – problems and perspectives. Indian Journal of Geology 60, 111–136.

Mancktelow, N.S., Pennacchioni, G., 2004. The influence of grain boundary fluids on the microstructure of quartz – feldspar mylonites. Journal of Structural Geology 26, 47–69.

Marchildon, N., Brown, M., 2002. Grain-scale melt distribution in two contact aureole rocks: implication for controls on melt localization and deformation. Journal of Metamorphic Geology 20, 381–396.

McLaren, A.C., Pryer, L.L., 2001. Microstructural investigation of the interaction and interdependence of cataclastic and plastic mechanisms in feldspar crystals deformed in the semi-brittle field. In: Boland, J., Ord, A. (Eds.), Deformation Processes in the Earth's Crust. Tectonophysics, 335, pp. 1–15.

Morse, S.A., Nolan, K.M., 1984. Origin of strongly reversed rims on plagioclase in cumulates. Earth and Planetary Science Letters 68, 485–498.

Mukherjee, A.B., 1989. P-T time history and thermal modeling of an anorthosite-granulite interface, Eastern Ghats metamorphic belt, India. In: Daly, J.S., Cliff, R.A., Yardley, B.W.D. (Eds.), Evolution of Metamorphic Belts. Geological Society, London, Special Publications, vol. 43, pp. 265–274.

Mukherjee, A.B., Bhattacharya, A., Chakravorty, S.C., 1986. Convergent phase equilibria at the anorthosite-granulite interface near Bolangir, Orissa, India and thermal evolution of a part of the Indian shield. Precambrian Research 34, 69–104.

Mukherjee, A.B., Jana, P., Das, S., 1999. The Banpur-Balugaon and Bolangir Anorthosite Diapirs of the Eastern Ghats, India: implications for the Massif Anorthosite Problem. Geology Review 41, 206–242.

Nicolas, A., 1992. Kinematics in magmatics rocks with special reference to gabbros. Journal of Petrology 33, 891–915.

Nicolas, A., Ildefonse, B., 1996. Flow mechanism and viscosity in basaltic magma chambers. Geophysical Research Letters 23, 2013–2016.

Park, Y., Means, W.D., 1996. Direct observation of deformation processes in crystal mushes. Journal of Structural Geology 18, 847–858.

Park, Y., Means, W.D., 1997. Crystal rotation and growth during grain flow in a deforming crystal mush. In: Sengupta, S. (Ed.), Evolution of Geological Structure in Macro- to Micro Scales. Charman and Hall, London, pp. 245–258.

Paterson, S.R., Fowler, T.K., 1993. Re-examining pluton emplacement processes. Journal of Structural Geology 15, 191–206.

Paterson, S.R., Vernon, R.H., Tobisch, T.H., 1989. A review of criteria for the identification magmatic and tectonic foliations in granitoids. Journal of Structural Geology 11, 349–363.

Paterson, S.R., Fowler Jr., T.K., Schmidt, K.L., Yoshinobu, A.S., Yuan, E.S., Miller, R.B., 1998. Interpreting magmatic fabric patterns in plutons. Lithos 44, 53–82.

Poirier, J.P., 1985. Creep of Crystals. High Temperature Deformation Processes in Metals, Ceramics and Minerals. Cambridge University Press.

Prasad, S., Bhattacharya, A., Raith, M.M., Bhadra, S., 2005. The origin of orthopyroxene/biotite + plagioclase coronas from the Bolangir anorthosite complex (India), and implications for reconstructing P-T paths. American Mineralogist 90, 291–303.

Raith, M., Bhattacharya, A., Hoernes, S., 1997. A HSFE and REE-enriched ferrodiorite suite from the Bolangir Anorthosite Complex, Eastern Ghats Belt, India. Proceedings of Indian National Academy of Science (Earth and Planetary Sciences) 106, 299–311.

Ramakrishnan, M., Nanda, J.K., Augustine, P.V., 1998. Geological evolution of the Proterozoic Eastern Ghats Mobile Belt. Geological Survey of India. Special Publication 44, 1–21.

Reesor, J.E., 1958. Dewar Creek Map-Area with special emphasis on the White Creek batholith. British Columbia. Memoir of the Geological Survey of Canada, 292.

Rosenberg, C.L., 2001. Deformation of partially-molten granite: a review and comparison of experimental and field investigations. The International Journal of Earth Sciences 90, 60–76.

Rosenberg, C.L., Handy, M.R., 2000. Syntectonic melt pathways during simple shearing of a partially-molten rock analogue (norcamphor-benzamide). Journal of Geophysical Research 105, 3135–3149.

Rosenberg, C.L., Riller, U., 2000. Partial melt topology in statically and dynamically recrystallized granite. Geology 28, 7–10.

Rosenberg, C.L., Stűnitz, H., 2003. Deformation and recrystallisation of plagioclase along a temperature gradient: an example from the Bergell tonalite. Journal of Structural Geology 25, 289–408.

Rybacki, E., Dresen, G., 2000. Dislocation and diffusion creep of synthetic anorthite aggregates. Journal of Geophysical Research 105, 26017–26036.

Rybacki, E., Dresen, G., 2004. Deformation mechanism maps for feldspar rocks. Tectonophysics 382. 193–187.

Sawyer, E.W., 2001. Melt Segregation in the continental crust: distribution and movement of melt in anatectic rocks. Journal of Metamorphic Geology 19, 291–309.

Stűnitz, H., Fitz Geraland, J.D., Tullis, J., 2003. Dislocation generation, slip systems and dynamic recrystallisation in experimentally deformed plagioclase single crystals. Tectonophysics 372, 215–233.

Tullis, J.A., 1983. In: Ribbe, P.H. (Ed.), Deformation of feldspars. Feldspar Mineralogy, Mineral. Soc. Am. Short Course Notes, 2, pp. 297–323.

Tullis, J., Yund, R., 1985. Dynamic Crystallization of feldspar: a mechanism for ductile shear zone formation. Geology 13, 238–241.

Tullis, J., Yund, R., 1991. Diffusion creep in feldspar aggregates: experimental evidence. Journal of Structural Geology 13, 987–1000.

Tullis, J., Yund, R.A., 1992. The brittle-ductile transition in feldspar aggregates: an experimental study. In: Evans, B., Wong, T.-F. (Eds.), Fault Mechanics and Transport Properties of Rocks. Academic Press, NY, pp. 89–118.

Tullis, J., Yund, R.A., Farver, J., 1996. Deformation-enhanced fluid-distribution in feldspar aggregates and implications for ductile shear zones. Geology 24, 63–66.

Urai, J.L., Means, W.D., Lister, G.S., 1986. In: Hobbs, B.E., Heard, H.C. (Eds.), Dynamic Recrystallisation of Minerals, Mineral and Rock Deformation: Laboratory Studies (The Paterson Volume). American Geophysical Union Geophysical Monograph, 36, pp. 161–199.

Vander-Voort, G.F., Gokhale, A.M., 1992. Comments on "Grain size measurements using the point sampled intercept technique". Scripta Metallurgica et Materialia 26, 1655–1666.

Vernon, R.H., 2004. A Practical Guide to Rock Microstructure. Cambridge University Press, 594 p.

Vernon, R.H., Williams, V.A., D'Arcy, W.F., 1983. Grain size reduction and foliation development in a deformed granitoid batholith. Tectonophysics 92, 123–145.

Vernon, R.H., Etheridge, M.A., Wall, V.J., 1988. Shape and microstructure of macrogranitoid enclaves: indicator of magma mingling and flow. Lithos 22, 1–22.

Vernon, R.H., Johnson, S.E., Melis, E.A., 2004. Emplacement-related microstructures in the margin of a deformed tonalite pluton: the San José pluton, Baja California, México. Journal of Structural Geology 26. 1887–1884.

Wang, Z.-C., Dresen, G., Wirth, R., 1996. Diffusion creep of fine grained polycrystalline anorthite at high temperature. Geophysical Research Letters 23, 3111–3114.

Wilkinson, D.S., Caceres, C.H., 1984. On the mechanism of strain-enhanced grain growth during superplastic deformation. Acta Metallurgica 32, 1335–1345.